

Pictures to: 3.4.1 Weak Beam Contrast of Stacking Faults in TEM

The set of pictures contained in the [publication](#) follows:

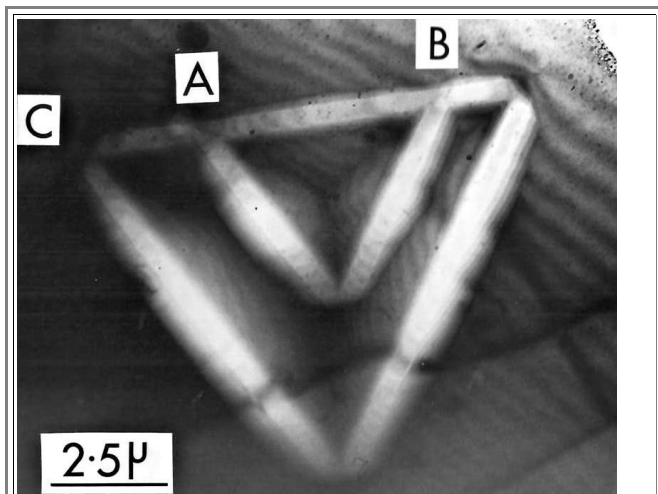


Fig. 1. 1.
Low magnification micrograph of the stacking faults in silicon which are studied in detail.

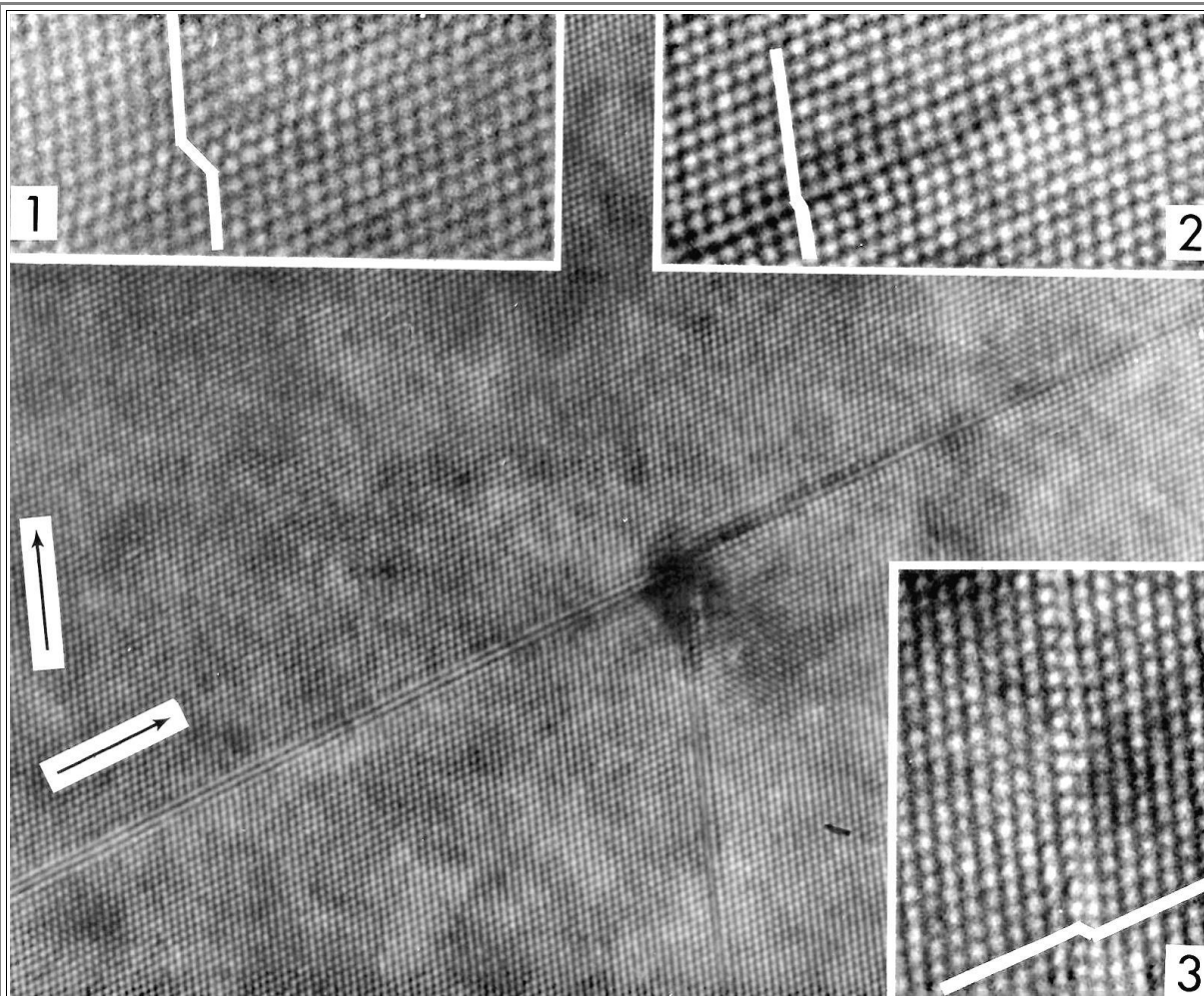
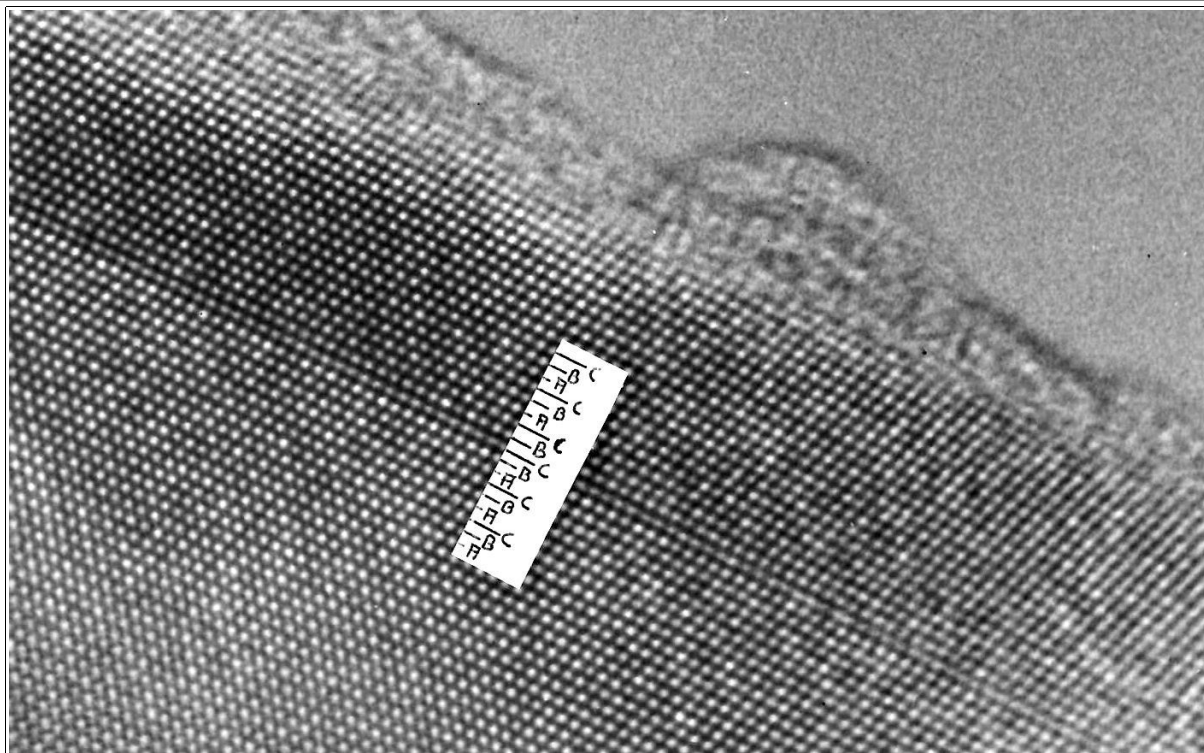
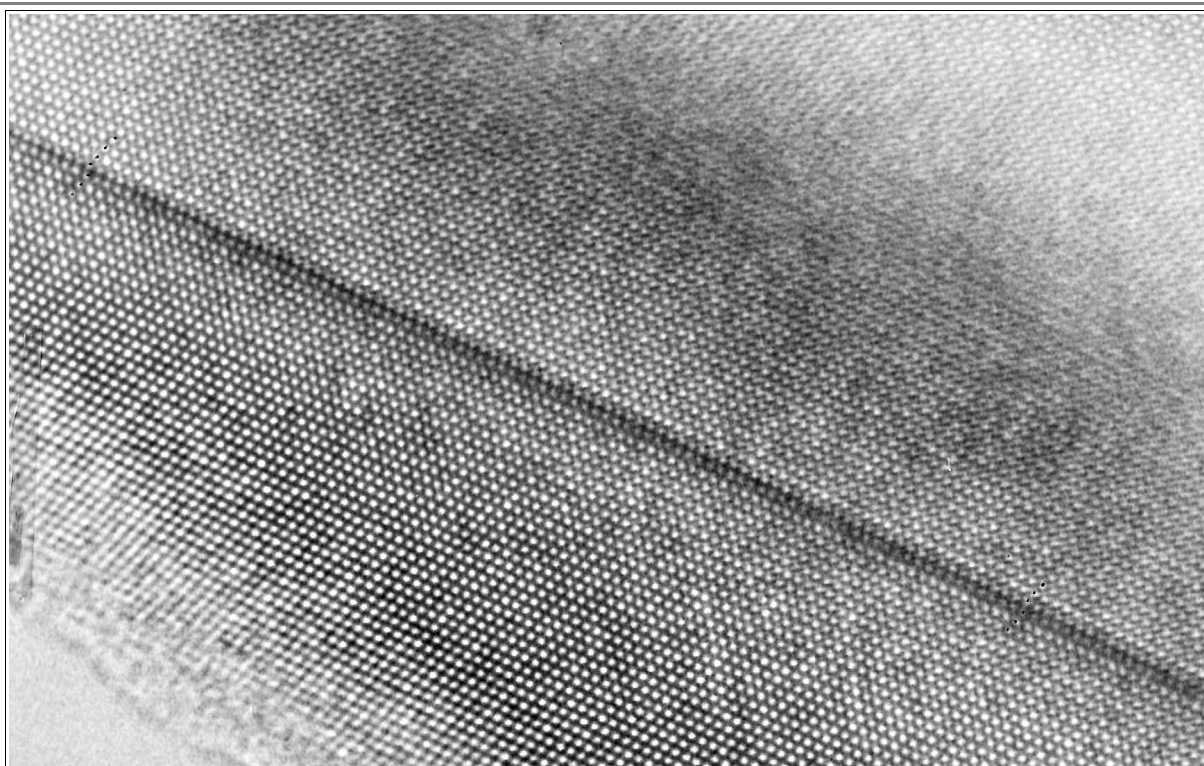


Fig. 2 .
Lattice image of stacking faults at area B in Fig. 1. Arrows denote traces of {111} planes.



Auxiliary picture to Fig Fig. 2

Showing parts of the stacking fault and illustrating the resolution one could achieve with the [Elmiskop](#) [102](#)



As above; auxiliiliary picture to Fig. 2

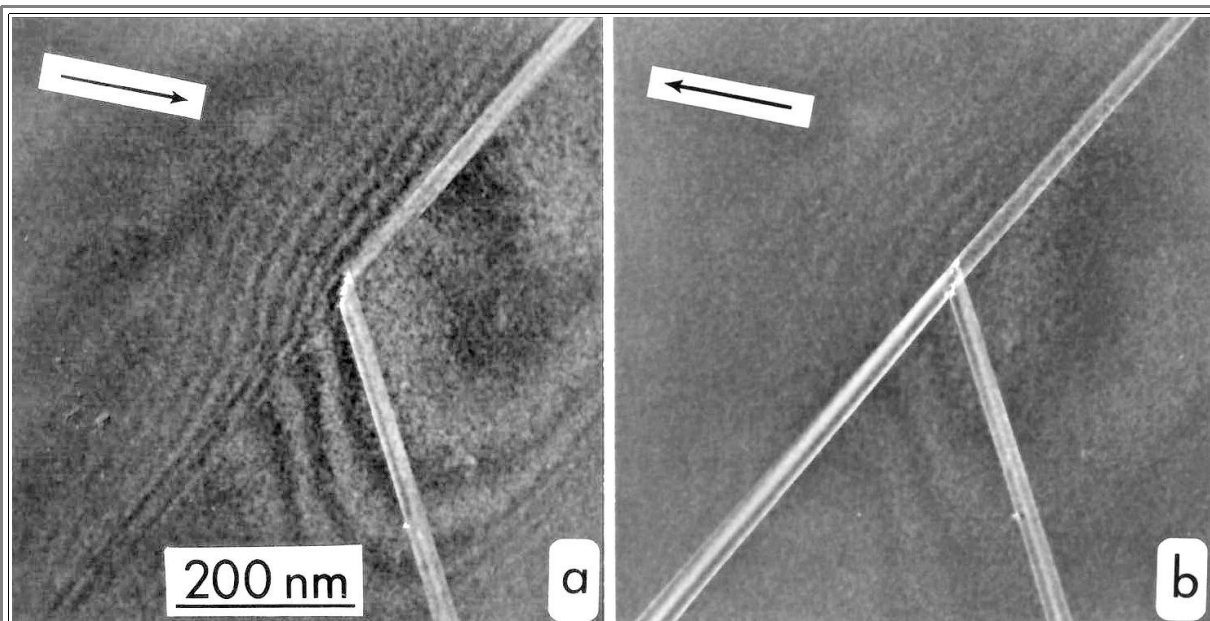


Fig. 3 .
Weak-beam image of area B. Arrows in this and in the following pictures indicate diffraction vectors.
 $g=\{220\}$ in this case

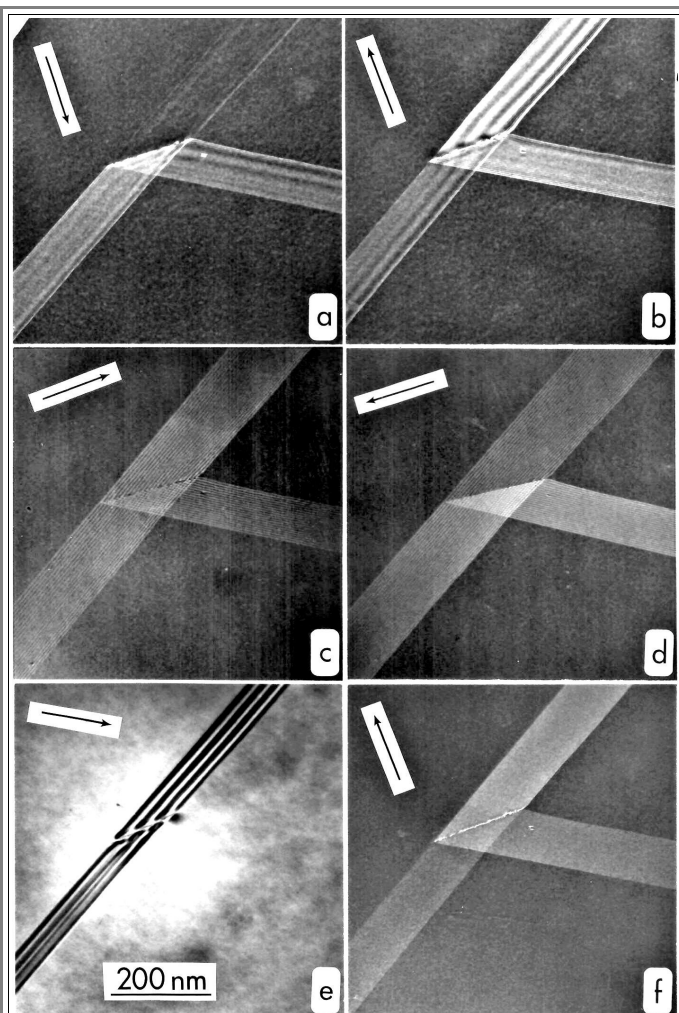


Fig. 4 .
Area A imaged with different diffraction vectors. a), b), c), f): $g=\{220\}$, c), d): $g=\{111\}$. For details see text

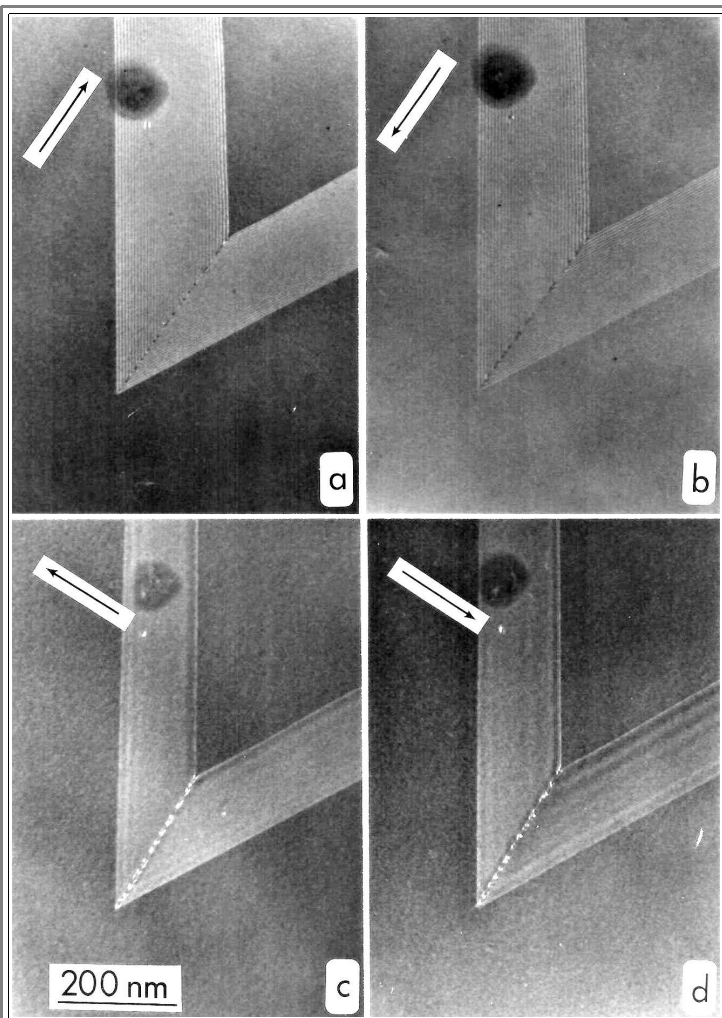


Fig. 5.
Area C imaged with different diffraction vectors. a), b): $y=\{111\}$;
c), d): $g=\{220\}$

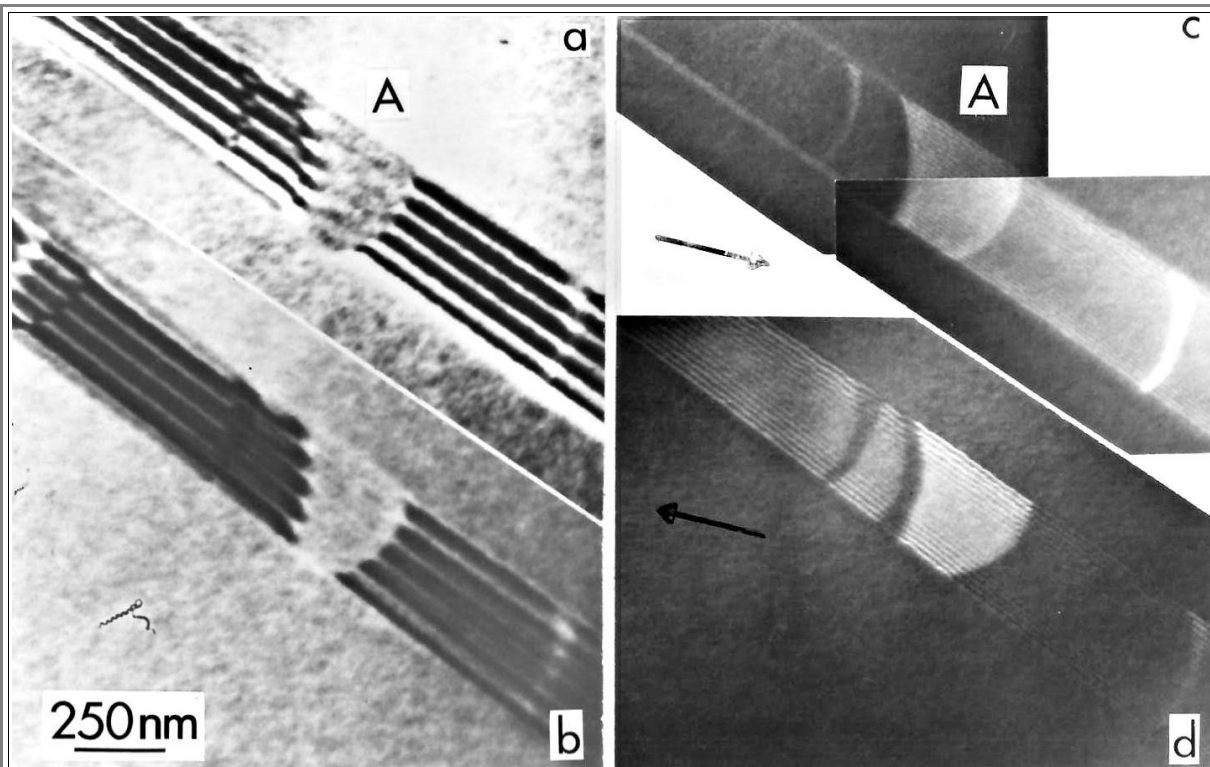


Fig. 6 This is a picture from B. Carter.
Overlapping stacking faults in stainless steel. The small arrows mark identical areas; $g=\{111\}$

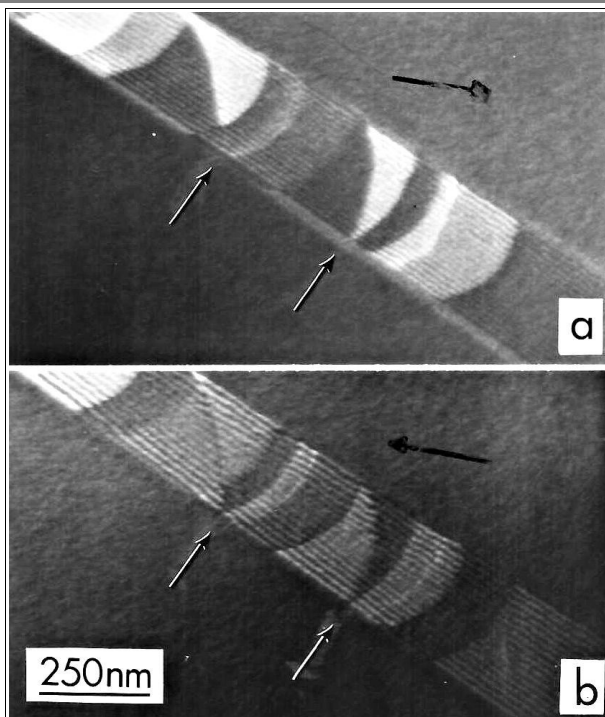


Fig. 7.

This is a picture from B. Carter.
Overlapping stacking faults in stainless steel. The small arrows mark identical areas; $g=\{111\}$

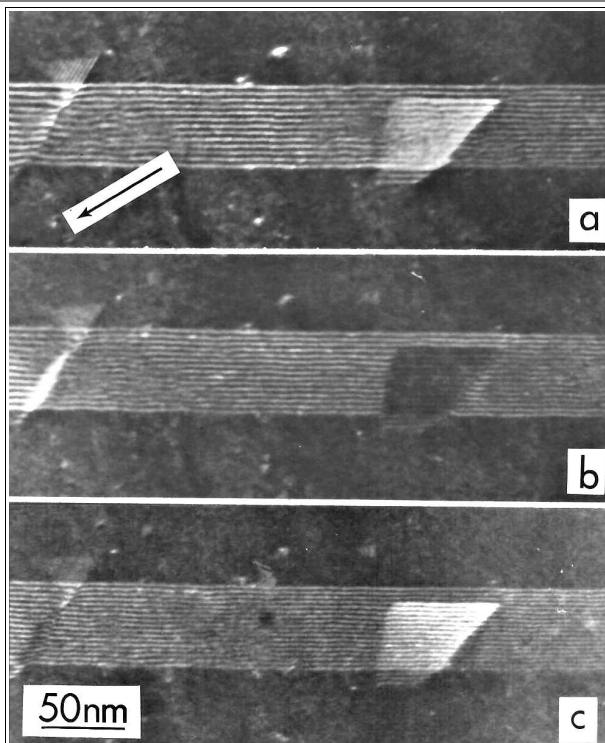


Fig. 8.

This is a picture from B. Carter.
Overlapping stacking faults in CuAl alloy. The magnitude of the excitation error s increases from a) to c; $G=\{111\}$

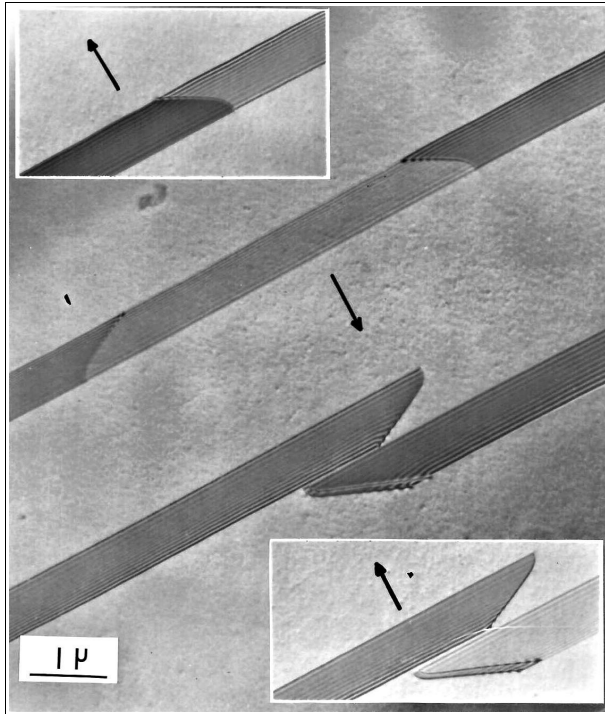


Fig. 9.

This is a picture from B. Carter.

Overlapping stacking faults in Si. A significant contrast change is visible upon reversing the sign of $g=\{220\}$ as shown in the inserts